Pre-heating boiler feedwater for expanded cork agglomerate production using a parabolic trough system

Cite as: AIP Conference Proceedings **2033**, 150002 (2018); https://doi.org/10.1063/1.5067155
Published Online: 08 November 2018

António Castro, João P. Cardoso, Luís Filipe Mendes, Pedro Azevedo, and João Farinha Mendes

Pre-heating Boiler Feedwater for Expanded Cork Agglomerate Production Using a Parabolic Trough System

António Castro[1,2], João P. Cardoso[2,a)], Luís Filipe Mendes[1,b)], Pedro Azevedo[2,c)] and João Farinha Mendes[2,d)]

[1]*Instituto Superior Técnico, Universidade de Lisboa, Av. Rovisco Pais, 1049-001 Lisboa, Portugal.*
[2]*Laboratório Nacional de Energia e Geologia, Estrada do Paço do Lumiar 22, 1649-038 Lisboa, Portugal.*

[a)]Corresponding author: joao.cardoso@lneg.pt
[b)]filipe.mendes@tecnico.ulisboa.pt
[c)]pedro.azevedo@lneg.pt
[d)]farinha.mendes@lneg.pt

Abstract. The production of expanded cork agglomerate involves significant heat demand, requiring superheated steam at temperatures ranging from 300ºC to 370ºC. The energy required to this process can be suitably provided by concentrating solar thermal collectors. This work considers the thermal energy needs of a real plant, presenting the technical and economical analysis performed for a solar heat for industrial process system using parabolic trough collectors to preheat the feedwater used by the boiler providing steam to the expanded cork agglomerate production process.

INTRODUCTION

Cork is a natural product obtained from the outer bark of the cork oak tree (*Quercus suber*). Native from the Mediterranean area, most of its cultivation and industrial processing is located in Portugal and Spain, the major cork producers in the world, responsible for more than 80% of all the cork exports [1, 2, 3]. Cork is used in several applications, such as stoppers for alcoholic beverages, thermal, acoustic and vibratory insulation, decoration and furniture, clothing, and in automotive and aeronautic industry [4].

The industrial processing of cork encompasses a wide range of processes, some of which require heat at low and medium temperatures. Its thermal energy demand can be satisfied by solar thermal systems, presenting potential for integration with concentrating solar thermal (CST) technologies. The most common thermal processes in the cork industry are: cork boiling, cork drying and expanded cork agglomerate production.

The production of expanded cork agglomerate (ECA, also known as insulating cork board, ICB) involves significant heat demand, considering the requirement of steam at more than 300ºC in part of the manufacture process. The procedure is based on the secretion of cork's natural resins and the expansion of the cork granules by using water vapour at temperatures above 300ºC, without resorting to glues or additives or any materials other than cork. To generate the required steam, ECA production facilities are equipped with steam boilers burning biomass or fossil fuels.

This paper presents the technical and economical analysis performed for a solar heat for industrial process (SHIP) system using parabolic trough collectors to preheat the feedwater from the steam boiler used in the ECA production process, considering the case of a manufacturing facility located in the Santarém region in Portugal.

SolarPACES 2017
AIP Conf. Proc. 2033, 150002-1–150002-9; https://doi.org/10.1063/1.5067155
Published by AIP Publishing. 978-0-7354-1757-1/$30.00

CST INTEGRATION IN THE ECA INDUSTRIAL PROCESS

ECA Manufacturing Process

The cork used as raw material originates from low quality non-boiled cork that is unsuitable as raw material to other cork products (e.g. wine stoppers). The ECA production process begins with the preparation of the raw material, through a set of grinding and cleaning stages, in order to obtain cork granulate with particle size within the range of 5-20 mm (adjustable according to the desired properties of the agglomerate being produced). In some facilities this granulate can be further subject to a drying process before storage [5]. The resulting cork granules are subject to a thermochemical treatment within an autoclave. During this step the granules are placed within an autoclave and heated during 17 to 30 minutes by superheated steam which is injected in the autoclave at temperatures ranging from 300°C to 370°C and gauge pressures ranging from 30 to 60 kPa [1, 5]. Afterwards the resulting ECA blocks are cooled down and subject to mechanical processing (e.g. cutting or turning) in order to obtain the desired shape.

Energy Demand

A real facility entirely dedicated to the ECA production was considered as case study. Technical visits to the facility were performed to gather data from the steam generation process and to determine the thermal energy demand of the ECA manufacturing process, crucial for the analysis of the integration of parabolic trough collectors in the system.

In this particular case there is no granulate drying and process steam is produced by a biomass boiler, powered by cork powder (and some wood used for the start-up procedure). Due to the high quantity of dissolved contents in the steam exiting the autoclaves (organic compounds from the cork) the facility steam circuit operates in an open loop, with a constant influx of fresh feedwater from an underground aquifer. The feedwater is filtered and chemically treated, being stored in two buffer tanks (with a total volume of 16.5 m^3) before being pumped to the boiler, with an average mass flow rate of 1.41 kg s^{-1}. The boiler's furnace operation warms significantly the air of the boiler room which in turn heats the water stored at the buffer tanks. Considering the measurements performed at the site it is estimated that the water pumped to the boiler is on average at 21°C.

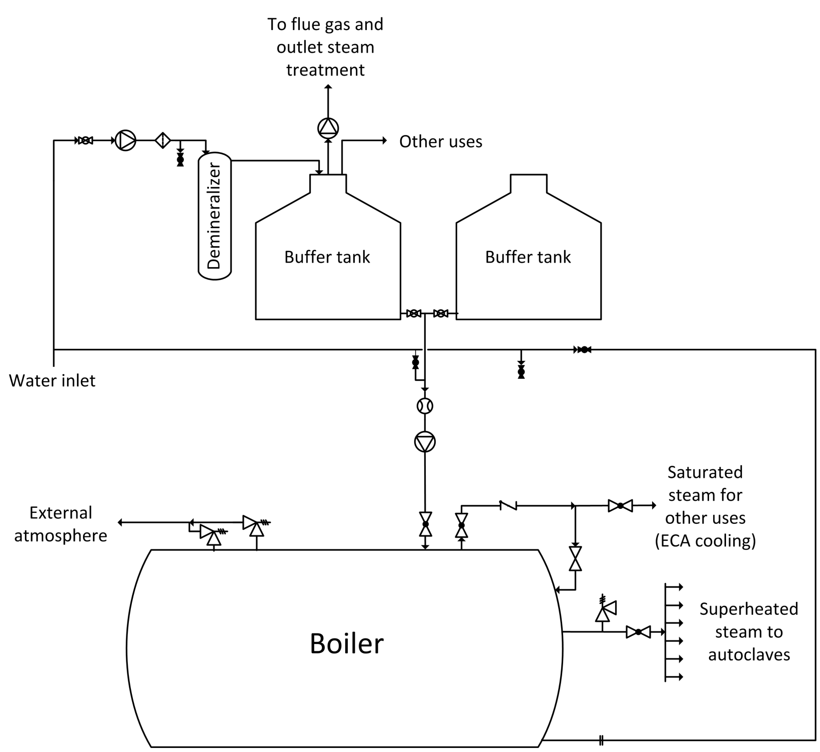

FIGURE 1. Simplified hydraulic scheme of the boiler circuit (valves coloured in black are closed during operation).

The steam boiler unit produces saturated steam at an average pressure of 8.2 bar. A small share of the produced steam is extracted to the ECA block cooling system. The majority of the saturated steam goes through a throttling valve, decreasing steam pressure to the required process pressure (around an average of 4.2 bar for this facility), before entering a superheater where it is superheated up to the required process temperature (with an average value of 354°C). A layout of the boiler circuit is presented in figure 1.

Long term data was available for the daily feedwater consumption. Considering the typical number of daily hours of operation it was possible to estimate the daily average value for the flow rate. Figure 2 presents the resulting average mass flow rate for the period between July 2015 and August 2016. Clearly visible are the vacation seasons during which the production is stopped.

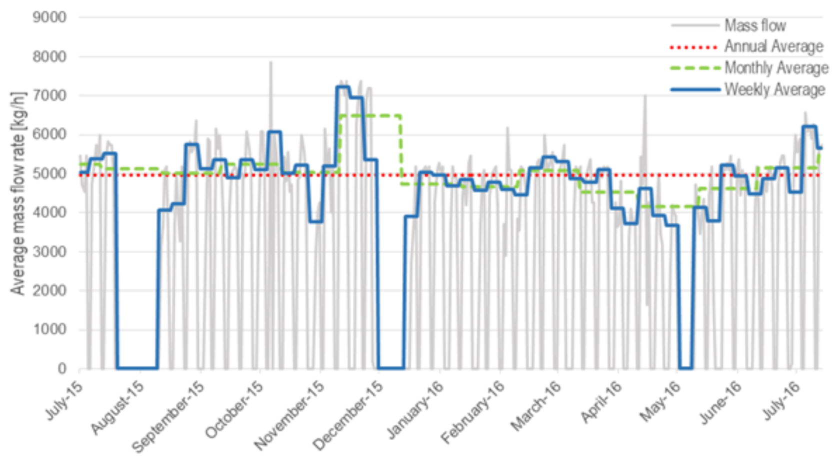

FIGURE 2. Feed-water mass flow rate average values considering different averaging periods.

Considering the previous information the thermal power demand for each boiler stage was estimated following thermodynamic principles. This information is presented in table 1 along with the boiler's annual thermal energy demand.

TABLE 1. Thermal power demand estimated for nominal operation and annual thermal energy demand of the ECA production process.

	Total	Pre-heating	Vaporization	Superheating
$\dot{Q}$ [kW]	4356	899	2882	575
Q [MWh]	9953	2052	6588	1313

Solar Thermal System

Solar thermal energy can be supplied by concentrating solar collectors to power the feedwater pre-heating, vaporization, steam superheating or a suitable combination of these processes.

Small parabolic trough collectors or linear Fresnel reflector systems able to achieve temperatures up to 200°C can be considered for the feedwater pre-heating application. A solar thermal system was designed in order to provide heat for the boiler's feedwater pre-heating process. This system is composed by two main circuits. In the first circuit (designated as solar circuit), cold heat transfer fluid (HTF) is pumped from the bottom of a buffer tank through a solar field composed by parallel loops of serially connected parabolic trough collectors. If the temperature of the HTF exiting the solar field is high enough it is temporarily stored in a buffer tank, otherwise it is redirected towards the solar field by a diverter valve. In the second circuit (process circuit) hot HTF is pumped from the buffer tank top through the hot side of the feedwater pre-heater heat exchanger, heating the boiler's feedwater before returning to the tank. The simplified scheme of the solar thermal system is discernible from figure 3.

PERFORMANCE ANALYSIS

Solar Pre-heating System Model

A TRNSYS [6] model was developed in order to assess the behaviour and annual performance of the solar feedwater pre-heating system. The model layout can be seen in figure 3 and its main components are stated in table 2.

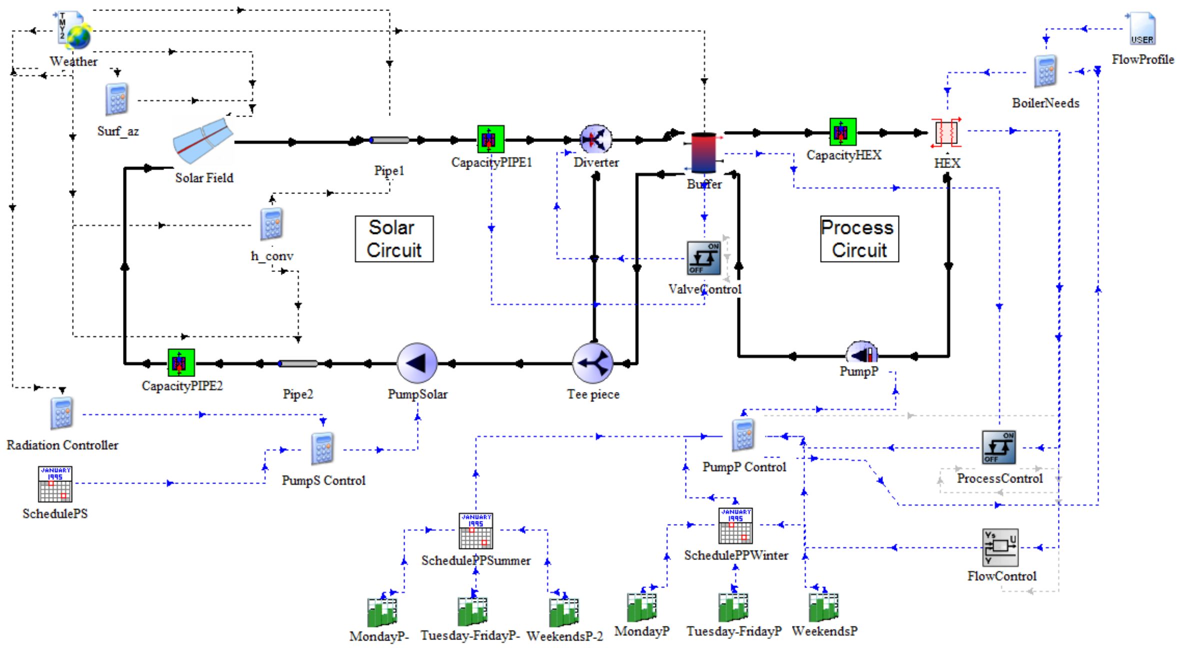

FIGURE 3. Trnsys model layout of the boiler's feedwater solar pre-heating system.

For the purposes of this work NEP SOLAR PolyTrough 1800 collectors have been considered with the dimensions and performance parameters given by [8] and [9] respectively. The PolyTrough 1800 collector is able to use thermal oil or pressurized water as HTF. For this performance analysis Therminol® 66 was chosen as HTF and the fluid properties given by [10] were used.

The solar field pump imposes a constant HTF mass flow rate equal to the nominal flow rate of the solar field (0.47 kg s^{-1} per parallel loop). It operates whenever the direct normal irradiance is greater than 100 W m^{-2} unless the day corresponds to Summer or Winter holidays. The temperature of the solar field HTF entering the buffer tank is controlled by a bypass valve which diverts the HTF from the tank to the solar field if the HTF temperature at the outlet of the solar field is lower than the temperature at the tank bottom. Additionally, whenever the HTF exiting the solar field has temperature higher than 250°C the solar collectors start to defocus in order to protect the system.

The process circuit pump modulates the HTF mass flow rate passing through the heat exchanger in order to achieve the desired temperature in the feedwater entering the boiler. The pump operation schedule follows the plant's boiler daily operation schedule, however, it only starts pumping if the temperature difference between the top of the buffer tank and the feedwater temperature at the entrance of the heat exchanger is higher than 15°C. When this temperature difference drops below 8°C or the boiler feedwater at the outlet of the heat exchanger reaches 171°C (risking vaporization outside of the boiler) the pump shuts down. If the feedwater outlet temperature reaches 170°C the pump speed is reduced in order to avoid overheating the feedwater and intermittent operation, particularly when process loads differ from the design point.

Hourly meteorological data for the plant location is provided by a TMY2 file generated with the Meteonorm software [11]. For this site annual direct normal irradiation reaches 2037 kWh m^{-2}, with a maximum monthly value of 278 kWh m^{-2} in July and a minimum of 100 kWh m^{-2} in December. Dry bulb air temperature oscillates between a maximum value of 35°C and a minimum of 2°C, averaging at approximately 16°C.

TABLE 2. TRNSYS model main components.

Name	Type	Description	Function
Solar Field	536	Parabolic Trough Solar Field	Models a North-South parabolic trough collector field, yielding temperatures and energies following the methodology presented in [7]
HEX	5b	Counterflow Heat Exchanger	Feedwater pre-heating with solar energy
PumpSolar	114	Single Speed Pump	Imposes the HTF mass flow rate in the solar circuit
PumpP	110	Variable Speed Pump	Imposes the HTF mass flow rate in the secondary circuit according to the feedwater temperature at the heat exchanger outlet
Weather	109	Data reader and radiation processor	Reads and processes the meteorological file providing radiation, temperature, wind velocity and solar angle values
Capacity (PIPE1, PIPE2, HEX)	306	Lumped mass for capacitance effects	Accounts for the thermal capacity of components
Buffer	4e	Uniform losses storage tank with user designated inlets	Models a stratified buffer storage tank
Diverter	11f	Controlled flow diverter	Controls the mass flow rate of HTF entering the buffer tank or diverted towards the solar field
Tee piece	11h	Tee-piece	Joins the buffer tank HTF return and diverted flow in the solar circuit
Pipe (1 and 2)	709	Circular fluid -filled pipe	Models the thermal losses of fluid flowing in a pipe

System Thermal Performance

Simulations were performed using the TRNSYS model in order to study the annual performance of the proposed system for different configurations. A parametric study was performed in order to determine the influence of the solar field aperture area, the buffer tank volume and the heat exchanger size in the energy production and in the solar fraction. The range of the different variables considered in the parametric analysis was: solar fields with 6 to 12 parallel rows and 3 to 8 collectors in series per row; buffer tank specific volumes of 0, 12, 24, 48 and 96 l m^{-2}; and UA values from 68793 to 682104 kJ h^{-1} K^{-1}.

Figure 4 presents the useful energy delivered to the boiler's feedwater by the solar system during a typical year of operation for different solar field aperture areas, heat exchanger UA value and the two extreme buffer tank specific volumes considered in the parametric analysis. Analysing the results for variations of the heat exchanger size it is possible to conclude that greater heat exchanger's UA values yield more useful energy. However, this effect is small when compared with the effect of the aperture area and less relevant for lower specific storage volumes.

The energy delivered by the solar system to the boiler's feedwater and the energy dumped in the solar field due to defocusing can be seen in figure 5 for the parametric runs performed for an heat exchanger designed for a solar field with 6 parallel loops and mass flow rate equal to the nominal mass flow rate of the collectors (i.e., 682104 kJ h^{-1} K^{-1}). Increasing the number of collectors in series at each parallel loop (i.e. increasing the solar field aperture area) increases the energy delivered by the solar system. However, this increase is limited by the maximum operating temperature of the solar field and the feedwater maximum temperature, resulting in the defocusing of some of the collectors to avoid overheating the system. This can be seen in figure 5 by observing the increase of the energy lost due to solar field defocusing for higher solar field areas. Additionally the collector efficiency is reduced for higher operating temperatures. All these effects result in lower increases of useful energy for higher solar field areas (i.e. the system presents diminishing marginal productivity).

Regarding the effect of the buffer tank specific volume, figure 5 also shows that for higher specific volumes the amount of dissipated energy is reduced. This results from the fact that it is possible to use the buffer tank to store part of the excess energy, increasing the useful energy delivered by the system. The solar collector TRNSYS model does not count as dumped energy the energy lost during periods were the field is not operating. Thus, dumped energy

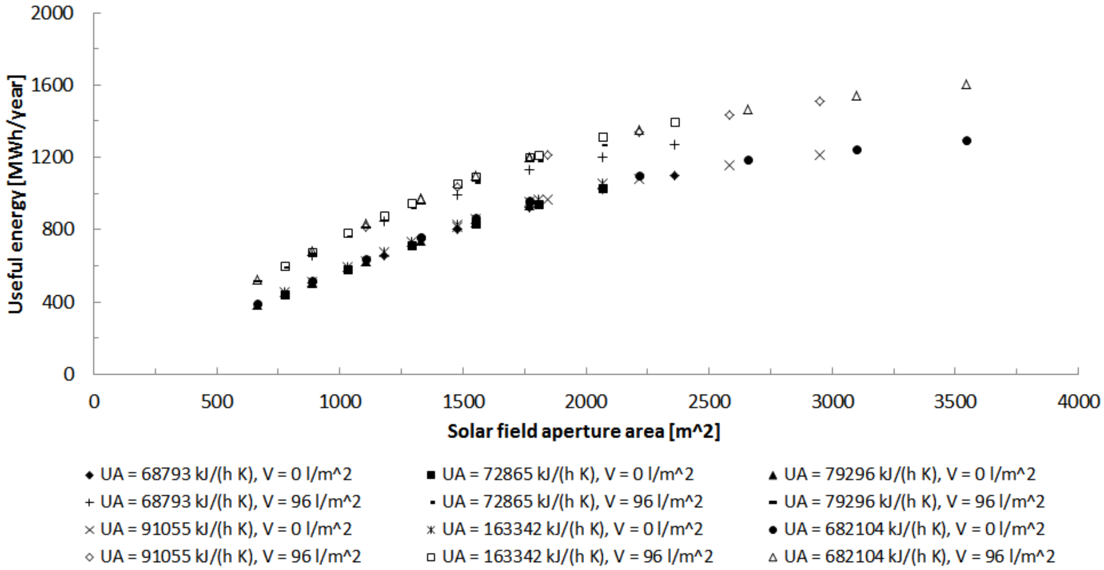

FIGURE 4. Useful energy delivered by the solar pre-heating system for variable solar field aperture areas and heat exchanger UA value, considering a buffer tank specific volume of 0 l m^{-2} (i.e, no tank) and 96 l m^{-2}.

values for the system without buffer case are not displayed since they are not comparable with the values obtained for the cases with buffer storage.

In the absence of the tank the energy delivered by the solar system to the feedwater is lower; however the energy lost to defocusing is also significantly lower.

System Economic and Environmental Performance

The investment costs related with the solar field (the collectors, solar field piping and support construction) were estimated to amount to 502.4 € m^{-2} of aperture area. This estimate is based on the information available for a solar heat for industrial process system installed in Switzerland at Emmi Dairy Saignelégier [12]. The costs related to the HTF correspond to Therminol® average market price of 5.75 € per kilogram as reported by the Eastman Chemical Company.

The investment costs for other components were estimated using available data from specialized chemical engineering design databases, namely the Matches online database [13] and the Cost Estimator Tool [14].

The total capital expenditure for the different systems considered in the parametric analysis varied between approximately 391 000 € and 3 725 000 €. The annual operation and maintenance costs for the different systems was estimated as 2% of the capital expenditure [15].

Assuming the investment costs are concentrated on the initial period, as well as constant operation and maintenance costs and useful energy production, the Levelized Cost of Heat (LCOH) can be computed as [16]:

$$LCOH = \frac{I_t(i + d_{om})}{E_{annual}} \tag{1}$$

where I_t represents the total investment costs, i the discount rate factor, d_{om} the operation and maintenance costs as a fraction of the total investment, and E_{annual} the energy provided by the system during one year of operation. The discount rate factor is a function of the risk free interest rate, the risk premium, the inflation rate and the lifetime of the project. For the purposes of this study the discount rate factor is valued at 7.29% for a 25 year period.

The LCOH value presents a small dispersion over the different sizes of the heat exchanger. In contrast, it is significantly more affected by the storage and solar field size - mostly due to the cost of the thermal oil stored in the tank and the solar field cost. For the set of system configurations considered in the study LCOH ranges from 0.089 € per kWh to 0.215 € per kWh, with an average value of 0.116 € per kWh. Figure 6 presents the LCOH for

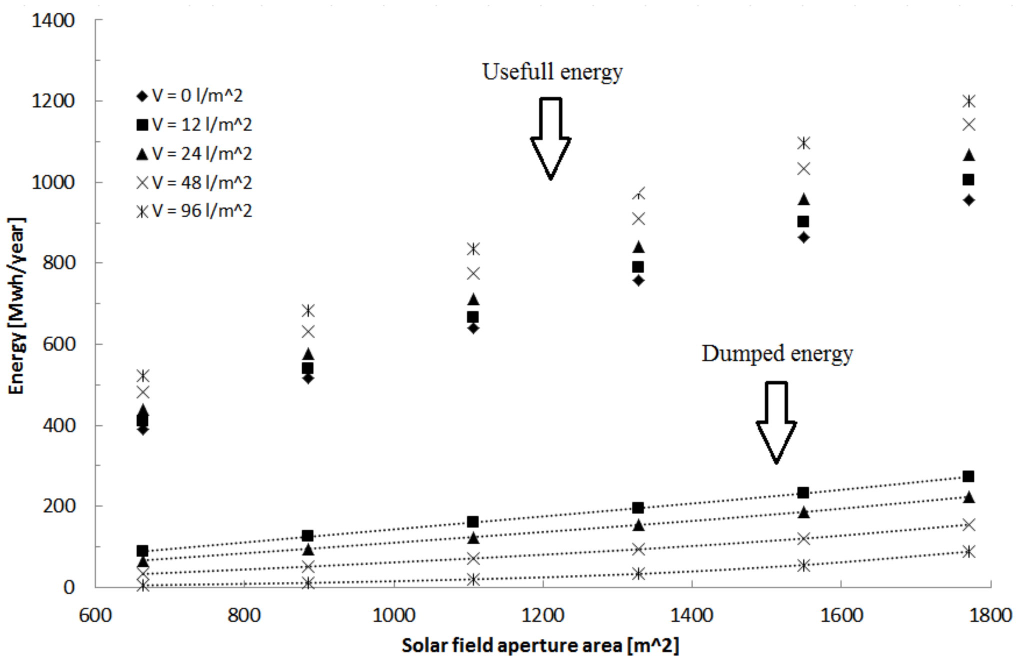

FIGURE 5. Useful energy delivered by the solar pre-heating system and energy dumped by the solar field through defocusing (dotted lines) for several solar field aperture areas and buffer tank specific volumes.

different buffer tank specific volumes and solar field areas for systems with a solar field composed by 6 parallel loops of collectors, which is the configuration were the lowest LCOH value is achieved.

There is an optimum value for the solar field size which minimizes the LCOH value. Increasing the buffer tank specific volume increases the LCOH and moves the minimum towards systems with smaller solar fields. The significant cost of the HTF used in the storage system is the main responsible for this behaviour, being the cost of larger storage tanks not sufficiently offset by the increased energy production. For the conditions of this study, the lowest LCOH (0.089 € per kWh) is found for a system without buffer storage, with a solar field composed by 6 parallel loops and 6 collectors in series per loop (total aperture area of 1328.4 m^2). According to the performed simulations, for a typical year, this system should deliver to the boiler's feedwater approximately 757 MWh of thermal energy, satisfying 7.61% of the energy needs of the boiler system (which corresponds to 36.9% of the energy needs for the feedwater pre-heating).

The figure also shows that for a given specific volume, the LCOH distribution near the optimum area is relatively flat, implying that small changes in the solar field area can be achieved without significant increase (or decrease) of the LCOH.

Although the industrial facility under consideration for this study uses cork powder to power its boiler, with the resulting greenhouse gas emissions considered to be null, saving cork powder allows it to be sold and used in other processes where it can displace the use of fossil fuels (such as the ones mentioned in [4]), reducing its consumption and the emission of greenhouse gases.

Not all ECA production facilities use biomass boilers. In order to assess the fossil fuel primary energy savings and the avoided greenhouse gas emissions due to the introduction of solar energy in the ECA production process a conventional system was defined, consisting of a LPG boiler with average efficiency of 85%. Primary energy conversion factors and greenhouse gases emission factors for LPG were considered to be 41868 MJ per tonne of oil equivalent (toe) and 63 $kg_{eq}CO_2\ GJ^{-1}$.

The use of solar thermal energy in the boiler's feedwater pre-heating yields, for the different systems considered in the parametric study, fossil fuel primary energy savings between 38.9 toe to 162.5 toe and greenhouse gases emissions avoided within the range of 102 729 $kg_{eq}CO_2\ GJ^{-1}$ to 428 663 $kg_{eq}CO_2\ GJ^{-1}$. Considering the system with the lowest LCOH, the estimative of the fossil fuel primary energy saving is 76.5 toe and 201 799 $kg_{eq}CO_2\ GJ^{-1}$ for the

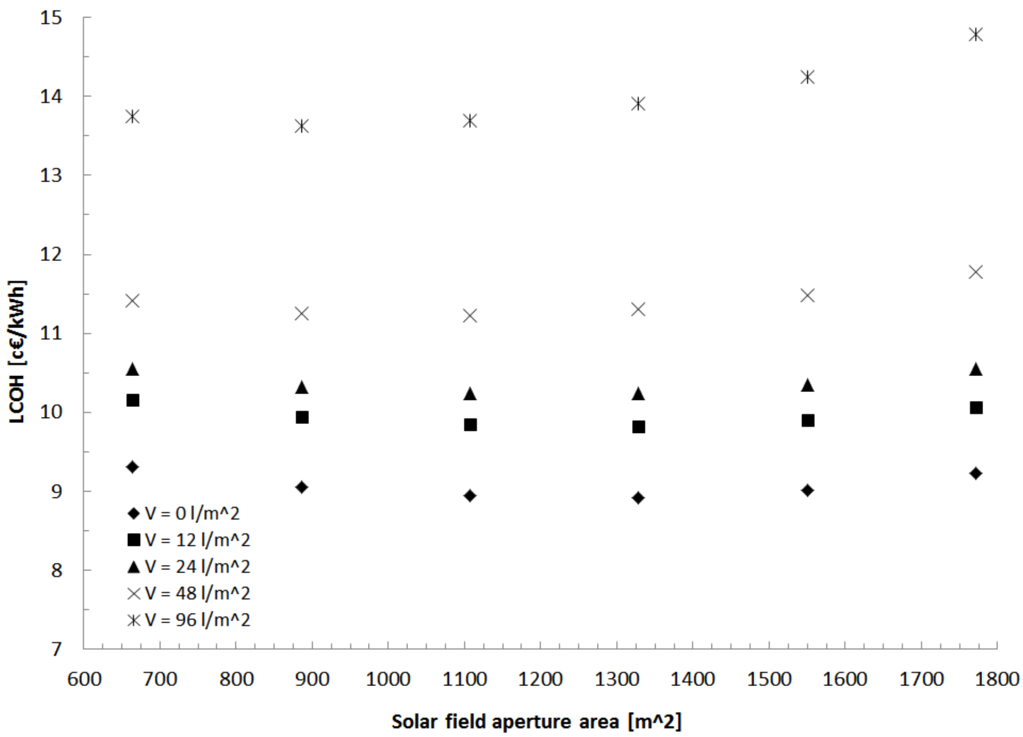

FIGURE 6. LCOH as a function of solar field aperture area and buffer tank specific volume for a solar field with 6 parallel loops.

avoidance of greenhouse gases emissions.

CONCLUSIONS

The design, modelling and simulation of a solar thermal system integrated into the feedwater pre-heating stage of the steam generation unit of an ECA production plant was performed, demonstrating the technical feasibility and potential of integrating solar process heat at the steam supply system of the ECA manufacture process.

The energetic and economic performance was analysed for different solar thermal systems. Several systems present LCOH values near the minimum, with the configuration minimizing the LCOH corresponding to a system without a buffer tank and with a solar field composed by 6 parallel loops and 6 collectors in series for each loop. Such system is able to provide (for the typical meteorological and productive year under consideration) thermal energy to the feedwater pre-heating at a cost of 8.92 € kWh^{-1}, with a total annual yield of approximately 757 MWh, satisfying around 36.9% of the energy consumed to preheat the boiler's feedwater, corresponding to around 7.6% of the total energy delivered by the boiler.

The systems under analysis all used thermal oil as HTF. However, for future works it will be interesting to analyse the use of water as HTF, either in a direct or indirect pre-heating system. This will imply a strong reduction in the storage costs, potentially moving the lowest LCOH system towards a configuration with storage.

ACKNOWLEDGMENTS

The research leading to these results has received funding from the European Union Seventh Framework Programme FP7/2007-2013 under grant agreement nº 609837.

REFERENCES

[1] H. Pereira, *Cork: Biology, Production and Uses* (Elsevier Science, 2007).

[2] L. Gil, Ciência e Tecnologia dos Materiais **25**, 38–41 (2013).

[3] F. Parejo, A. Branco, J. C. Lopes, and J. R. Preciado, in *Working Papers* (School of Economics and Management, Technical University of Lisbon, 2013) WP18/2013/DE/UECE/GHES.

[4] C. Barros, *Produção de Pellets para valorização de resíduos provenientes da indústria corticeira*, Master's thesis, Escola de Engenharia, Universidade do Minho (2013).

[5] L. Gil, *Cortiça: Produção, Tecnologia e Aplicação* (Instituto Nacional de Engenharia e Tecnologia Industrial, Lisboa, 1998).

[6] A TRaNsient SYstems Simulation Program, Solar Energy Laboratory, University of Wisconsin-Madison (version 17), URL: https://sel.me.wisc.edu/trnsys/.

[7] J. A. Duffie and W. A. Beckman, *Solar Engineering of Thermal Processes* (John Wiley and Sons, New Jersey, 2013).

[8] Technical data for the PolyTrough 1800, NEP Solar (version 7), URL: http://www.nep-solar.com/downloads/.

[9] Solar collector factsheet - NEP PolyTrough 1800, Solartechnik Prüfung Forschung, Institut für Solartechnik (2013), test report C1549 available at http://www.spf.ch.

[10] Therminol® 66 technical bulletin, Eastman Chemical Company (2013), URL: https://www.therminol.com/products/Therminol-66.

[11] Meteonorm, Meteotest (version 7.1), URL: http://www.meteonorm.com.

[12] Solar thermal plants database, AEE INTEC (2015), URL: http://ship-plants.info/solar-thermal-plants.

[13] Index of process equipment, Matches (2016), URL: http://www.matche.com/equipcost/EquipmentIndex.html.

[14] M. Peters, K. Timmerhaus, and R. West, Equipment costs - plant design and economics for chemical engineers, 2017, URL: http://www.mhhe.com/engcs/chemical/peters/data/.

[15] S. Kalogirou, Applied Energy **76**, 337–361 (2003).

[16] R. Castro, *Uma Introdução às Energias Renováveis: Eólica, Fotovoltaica e Mini-Hídrica* (IST Press, Lisboa, 2012).